Gas–Liquid Solubilities of the Methanol Synthesis Components in Various Solvents

Geert H. Graaf, Harrie J. Smit, Elze J. Stamhuis, and Anthonius A. C. M. Beenackers*

Department of Chemical Engineering, The University of Groningen, Nijenborgh 16, 9747 AG Groningen, The Netherlands

The solubilities of CO, CO_2, H_2, CH_3OH, and H_2O were measured in hexadecane, octadecane, squalane, and benzophenone at 293–573 K and 1.013–90 bar using volume displacement and material balance techniques. The experimental results, consisting of 260 solubility data for 16 binary mixtures, were used to test the applicability of four solubility models. When using literature model parameters, the Skjold-Jørgensen group-contribution equation of state gives the best agreement with the experimental results with an average deviation of 15%. The Soave–Redlich–Kwong and Peng–Robinson equations of state give an excellent agreement with the experimental results when optimized binary interaction coefficients are used. The regular solutions theory gives reasonable results except for the methanol- and water-containing systems when using no optimized binary parameters. Finally, our results show a reasonable agreement with the available literature data.

Introduction

In the last 10 years an increasing interest for slurry reactors has been developed. Two important examples are three-phase Fischer–Tropsch synthesis and three-phase methanol synthesis. For a good process design or process description involving slurry reactors, knowledge of the solubilities of the gaseous components in the slurry liquids is nearly always required. This holds in particular for processes in which mass transfer limitations in the slurry phase play a role. Despite the fact that gas–liquid solubilities may be regarded as so-called basic data for process engineering, these data are rather scarce at elevated temperatures and pressures as well as for solvents different from water. Moreover, theoretical models that can be used for predicting gas–liquid solubilities contain adjustable parameters, which have to be estimated from accurate experimental data.

The objectives of this paper are to present accurate experimental solubility data of all methanol synthesis components and to clarify what theoretical model (of a selected group of models) gives the best prediction of gas–liquid solubilities of interest in three-phase methanol synthesis. Furthermore, optimal adjustable parameters will be presented for these models, based on our experimental data.

Experimental Section

Equipment and Principles of Measurement. The solubility experiments were carried out with a low-temperature, low-pressure apparatus (LTLp) and with a high-temperature, high-pressure apparatus (HTHp). The principle of measurement for the LTLp apparatus is based on the measurement of the volume of gas dissolved in a known amount (by weight) of solvent. The LTLp apparatus primarily consists of a thermostated combination of a glass vessel connected with a horizontal, volume-calibrated glass tube. The measurement of the volume of gas dissolved is carried out by means of monitoring the location of a mercury drop in the glass tube throughout the dissolution process. A complete description of the LTLp solubility apparatus is given by Meuldijk et al. (*1*).

A schematic drawing of the HTHp solubility apparatus is given in Figure 1. The determination of the solubility is based on the measurement of the equilibrium pressure *p* at a chosen temperature *T* while the amounts of solute and solvent as well as the volumes of both phases are known. In fact, the solubility (e.g., Henry constant) is calculated from a material balance for the solute. Except for the dosing technique, our method is comparable with the one described by Olsen (*2*). Cukor and Prausnitz (*3*) also used an experimental technique based on the calculation of a material balance for the solute.

Gas–liquid equilibrium was established in a stainless steel bomb (1), which was shaken to improve the contact between the two phases. In order to make this movement effective, vertical baffles (2) were placed in the bomb. The bomb was tightened with an annealed copper ring (3). The pressure in the bomb was measured with a pressure transducer (4) (Brosa, type EBM 0520, 1500 psi). This pressure transducer was calibrated with an accurate manometer (5) (Wiegand, type 342.11, 0–160 bar, class 0.1, including calibration certificate). The estimated errors of the measured pressures (including reproducibility and systematic effects) are ±0.1 bar for the manometer (based on the test certificate) and ±0.2 bar for the pressure transducer (deviations between the manometer and the calibrated pressure transducer were within ±0.1 bar). The temperature in the bomb was measured with a Pt-100 resistance thermometer (6) (Sensing Devices Limited, four-coil type). The bomb was placed in a fluidized sand bed (7), which was thermostated by a PI thermal controller. The estimated error of the measured temperatures is ±0.3 K (including reproducibility and systematic effects). This value was estimated by comparing the thermometer with a standard (calibrated) Pt-100 thermometer and by measuring the freezing point of water and the normal boiling points of water and dodecane (literature values, respectively, 273.2, 373.2, and 489.5, Reid et al. (*4*)).

For the addition of CO, CO_2, and H_2 a supply cylinder (8) was used. The amount of solute fed to the bomb was determined by measuring the temperature (9) and the pressure (5) in the supply cylinder before and after the feeding while the volume of the supply cylinder was known accurately. A correction for nonideal gas behavior was made by using literature compressibility factors *Z* (*5*).

The amount of solvent added was determined by weight. Methanol and water (solutes) were introduced as liquids, and the amounts were also determined by weight. Weight measurements were carried out with a Mettler P120 balance (inaccuracy 0.01 g per reading) and a Mettler H10 balance (inaccuracy 0.1 mg per reading).

Degassing and venting of the system was possible using a three-way valve (10).

In order to be able to obtain phase-equilibrium information from the HTHp apparatus, it is necessary to know the volume of the bomb. Also the volume of the supply cylinder (together with the connection lines, valves, and manometer) is needed. Volume measurement was carried out by filling the relevant object with gas (helium or nitrogen) at a high pressure (>50 bar)

---

* To whom correspondence should be addressed.

0021-9568/92/1737-0146$03.00/0

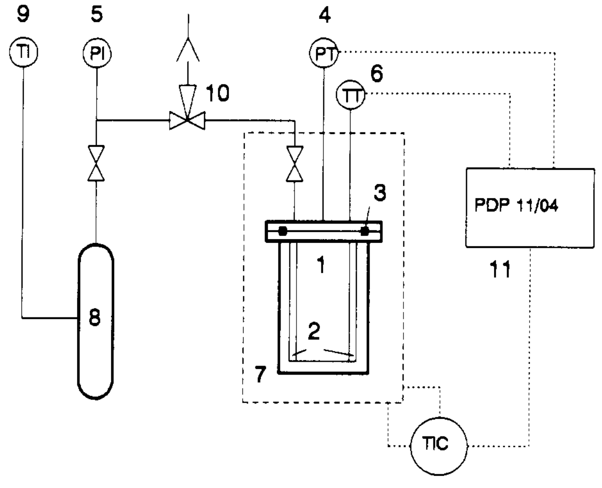

Figure 1. Schematic drawing of the high-temperature, high-pressure (HTHp) solubility apparatus: (1) bomb; (2) baffles; (3) copper ring; (4) pressure transducer; (5) manometer; (6) Pt-100 resistance thermometer; (7) fluidized sand bed; (8) supply cylinder; (9) thermometer; (10) three-way valve; (11) PDP 11/04 mini computer.

and subsequently purging the gas through a wet gas meter (Meterfabriek Schlumberger, type 1, inaccuracy 0.2%). From the measurement of p and T before (a) and after (b) this procedure, together with the amount of gas that has passed the gas meter, the vessel volume can be calculated. Here, the accurate manometer and a 0.1 K scale glass-in-tube thermometer were used to measure p_a, T_a, and T_b. For the measurement of p_b a mercury barometer was used. Corrections for nonideal gas behavior (which are small for helium and nitrogen at the relevant conditions) were made by using literature Z values (*5*). Interpolation of the tabulated Z values was carried out with the use of the Soave-Redlich-Kwong (SRK) equation of state (*6*) and by using effective (eff) values for the acentric factors ω (He, $\omega_{eff} = -0.394$ for $T = 288.15-323.15$ K and $p = 1-150$ bar; N_2, $\omega_{eff} = -0.017$ for $T = 280-300$ K and $p = 1-200$ bar). The critical properties were taken from Reid et al. (*4*) (He, $p_c = 2.27$ bar, $T_c = 5.19$ K; N_2, $p_c = 33.9$ bar, $T_c = 126.2$ K). This interpolation method allows for a very accurate reproducibility of the tabulated Z values (deviations <0.03%). The absolute error of the volume measurements is estimated to be 1 mL. This estimation was obtained by comparing the results of approximately 10 measurements per vessel with helium and nitrogen at various filling pressures (50–100 bar). The values of the volume of the bomb (at 293.2 K) and the supply cylinder were determined to be 508.0×10^{-6} and 353.8×10^{-6} m^3, respectively.

The measurements and the temperature control were automized with a PDP 11/04 mini computer (11). For the temperature control a proportional-integrating algorithm was written. The temperatures and the pressures in the bomb were measured at intervals of 5 min. It was assumed that equilibrium had been reached if five subsequent measurements were constant within 0.3 K and 0.1 bar, without showing a trend in the T and p data with time. The time necessary to reach these constraints was usually 1–2 h. The PDP 11/04 mini computer was programmed to carry out a series of experiments (for each solute–solvent combination), for example, starting at 423 K, moving up to 563 K with steps of 10 K, and going down again to 423 K with steps of 10 K. This "moving up–going down" method was employed in order to check whether the bomb was completely gas tight.

Table I. Experimental Conditions (Pressure p and Temperature T) for Measuring Solubility Data

solute–solvent	no. of experiments		p/bar		T/K	
	LTLp	HTHp	LTLp	HTHp	LTLp	HTHp
$CO-C_{16}H_{34}$	7		1.013		298–353	
$CO-C_{18}H_{38}$	7	14	1.013	30–38	303–353	433–563
$CO-C_{30}H_{62}$	10	15	1.013	24–35	293–353	423–563
$CO-C_{13}H_{10}O$	4	15	1.013	31–46	323–353	423–563
$CO_2-C_{16}H_{34}$	7		1.013		298–353	
$CO_2-C_{18}H_{38}$	9	15	1.013	19–30	303–353	423–563
$CO_2-C_{30}H_{62}$	11	15	1.013	24–41	293–353	423–563
$CO_2-C_{13}H_{10}O$	5	15	1.013	19–31	323–353	423–563
$H_2-C_{16}H_{34}$	7		1.013		293–353	
$H_2-C_{18}H_{38}$	6	13	1.013	50–64	303–353	443–563
$H_2-C_{30}H_{62}$	7	15	1.013	75–81	293–353	423–563
$H_2-C_{13}H_{10}O$	5	15	1.013	51–70	323–353	423–563
$CH_3OH-C_{30}H_{62}$		12		9–20		453–563
$CH_3OH-C_{13}H_{10}O$		9		10–21		463–563
$H_2O-C_{30}H_{62}$		11		10–15		463–563
$H_2O-C_{13}H_{10}O$		11		9–29		463–563

Table II. Source and Purity of Compounds

compound	source	purity/%
carbon monoxide	Hoekloos	>99
carbon dioxide	Hoekloos	>99.9
hydrogen	Hoekloos	>99.995
methanol	Merck-Schuchardt	>99.8
water	laboratory-made	>99.9
hexadecane	Janssen	99
octadecane	Aldrich	99
squalane[a]	Janssen	99
benzophenone	Merck-Schuchardt	99

[a] 2,6,10,15,19,23-Hexamethyltetracosane ($C_{30}H_{62}$).

Measurements. An overview of the experimental conditions is given in Table I, while Table II presents a summary of the chemicals used. The LTLp solubility apparatus is not suitable for measurements with condensable vapors such as methanol and water. For the HTHp solubility apparatus the accuracies of the experimental Henry constants are strongly dependent on the amount of solvent in the bomb. This is especially important for the measurements with CO, CO_2, and H_2: due to the dosing technique these measurements have a much lower accuracy than the measurements with H_2O and CH_3OH. For each series of experiments with the HTHp solubility apparatus, the optimal amount of solvent was calculated and employed. These calculations were based on the group-contribution equation of state (*7, 8*) to predict the solubility in combination with the error analysis which is presented later in this paper.

Because the volume of the solvent in the bomb is needed for the calculation of the solubility, the densities ρ of the solvents were measured with a Westphal balance (*9*) at temperatures between 293 and 563 K. At temperatures below 353 K the solvents were placed in a glass vessel heated by a water bath. At higher temperatures a small stainless steel vessel placed in a liquid metal bath was used. The temperature was controlled by a proportional-integrating controller, resulting in temperature deviations of less than 0.1 K. The volume of the displacement block was 2.5397×10^{-6} m^3. This value was determined by using the Westphal balance with doubly distilled water at 298.2 K ($\rho = 997.0$ kg m^{-3} (*10*)). The mass of the displaced liquid was determined by contraweights with an accuracy of ±0.0002 g. In order to obtain the overall measuring accuracy (with regard to ρ), several measurements were carried out with doubly distilled water (in the range 293–353 K) and some measurements (with the solvents investigated) were repeated. Hence, it was estimated that the overall experimental error is 0.5%.

The experimental densities, which are given in Table III, are correlated with the following equation.

$$\rho = a - b(T - 273.2) \qquad (1)$$

The deviations between the experimental and calculated values

Table III. Experimental Densities[a] ρ of Solvents as a Function of Temperature T and Coefficients a and b, Equation 1

hexadecane		octadecane		squalane		benzophenone	
T/K	ρ/(kg/m^3)	T/K	ρ/(kg/m^3)	T/K	ρ/(kg/m^3)	T/K	ρ/(kg/m^3)
374.6	718.7	303.2	772.7	293.2	807.3	329.2	1081.0
421.9	685.5	313.2	766.3	298.2	803.8	333.2	1078.8
469.4	650.0	323.2	759.7	303.2	800.8	343.2	1071.1
516.2	613.0	333.2	750.6	313.2	793.2	353.2	1061.5
537.5	599.2	343.2	744.5	323.2	783.7	373.2	1045.8
		353.2	735.2	333.2	778.3	423.2	1000.9
		372.4	727.0	343.2	770.3	474.7	956.5
		422.7	692.1	353.2	766.8	520.6	916.1
		476.1	657.7	373.9	755.0		
		521.8	622.6	374.0	756.6		
				418.7	726.5		
				470.2	692.1		
				524.7	655.4		
				561.6	631.0		
a = 794.8		a = 792.5		a = 819.1		a = 1131.0	
b = 0.74		b = 0.68		b = 0.65		b = 0.87	

[a] Estimated experimental error of the reported densities 0.5%. This error contains both reproducibility and systematic effects.

are very small: average deviations <0.2%, maximum deviations <0.5%. Furthermore, the residuals are normally distributed around zero.

In the calculations the value of the volume of the bomb was corrected for the effect of thermal expansion. The cubic thermal expansion coefficient was taken as 5.2×10^{-5} K^{-1} (*11*). The amount of gas in the bomb (mol) was calculated by using the Soave–Redlich–Kwong (SRK) equation of state (*6*).

Calculation of the Pseudoexperimental Henry Constants from the Experimental Results. Both the LTLp method and (especially) the HTHp method do not allow for a direct calculation of the experimental Henry constants H from the primary measurements. This is caused by the fact that the equations involved have to be solved iteratively. Moreover, some assumptions have to be incorporated in the calculation framework. The following methods and equations have been used.

LTLp Calculation Framework. The primary experimental data are T, p, the mass of solvent W_1, and the volume change ΔV.

The experimental Henry constant $H_{1,2}$ is given by

$$H_{1,2} = y_2\varphi_2 p/x_2 \qquad (2)$$

where

$$\varphi_2 = F(T,p,y_1,y_2) \qquad (3)$$

Here φ_2 is the fugacity coefficient of the solute in the vapor phase, x_2 the mole fraction of the solute in the liquid phase, and y_2 the mole fraction of the solute in the vapor phase. The function involved is based on the SRK equation of state (*6*).

SRK is also used for the calculation of the mole fraction of the solvent in the vapor phase y_1 and for the calculation of the compressibility factor in the vapor phase Z^V. The change in volume ΔV^{calc} is calculated from the following equation.

$$\Delta V^{calc} = \frac{x_2}{(1-x_2)}\frac{W_1}{M_1}\left[\frac{y_2RTZ^V}{p} - v_2^L\right] \qquad (4)$$

where M_1 is the molecular mass of the solvent and v_2^L the molar volume of the solute.

The calculation of ΔV contains the following assumptions. The change in liquid-phase volume is based on additivity in volume and constant v_2^L.

The change of liquid-phase volume due to vaporization (and condensation) of the solvent is neglected. This assumption is reasonable since we used only high-boiling solvents.

These calculations represent in fact very small corrections compared to those assuming ideal-gas behavior and zero vapor pressure of the solvent. It should be noted that zero binary interaction coefficients were used in these SRK calculations. This has no significant influence on the resulting pseudoexperimental Henry constants, which were checked afterward. A pseudoexperimental Henry constant is calculated iteratively. The iteration involves minimization of $\Delta V - \Delta V^{calc}$ toward zero.

HTHp Calculation Framework. The primary experimental data are p, T, W_1, p_a, T_a, p_b, and T_b for CO, CO_2, and H_2 and p, T, W_1, and W_2 for CH_3OH and H_2O.

The calculation framework for the HTHp results consists of eqs 2 and 3 together with

$$n_1 = W_1/M_1 \qquad (5)$$

where n_1 is the number of moles of the solvent, and

$$n_2 = \frac{V_{sc}}{R}\left[\frac{p_a}{T_aZ_a} - \frac{p_b}{T_bZ_b}\right] \qquad (6)$$

where n_2 is the number of moles of the solute provided by the supply cylinder and V_{sc} the volume of the supply cylinder. R is the gas constant. The subscript a means the initial conditions, b the final conditions. In the cases of methanol and water the number of moles of the solute is given by

$$n_2 = W_2/M_2 \qquad (7)$$

The compressibility factors Z_a and Z_b were calculated with SRK (*6*) using effective acentric factors (CO, $\omega_{eff} = -0.0195$; CO_2, $\omega_{eff} = 0.468$; H_2, $\omega_{eff} = -0.192$). These values allow for a very accurate interpolation of tabulated literature Z values (*5*).

$$n_2^L = \frac{n_1 - n_2y_1/y_2}{(x_1/x_2 - y_1/y_2)} \qquad (8)$$

$$n_2^V = n_2 - n_2^L \qquad (9)$$

$$n_1^L = n_2^Lx_1/x_2 \qquad (10)$$

$$n_1^V = n_1 - n_1^L \qquad (11)$$

$$V_{bomb}^{calc} = (M_1/\rho_1)n_1^L + v_2^Ln_2^L + v^V(n_1^V + n_2^V) \qquad (12)$$

$$v^V = RTZ^V/p \qquad (13)$$

In principle, the same assumptions are valid as reported for the LTLp calculation framework. However, the change in liquid-phase volume due to vaporization of the solvent is included, eq 12. The vapor pressure is calculated from SRK rather than from conventional methods (Lee–Kesler, Antoine, etc.) in order to take into account the increase of the vapor pressure due to

Table IV. Error Sources for the LTLp Experiments

param	origin	corresponding error	remarks
y_1	SRK	20%	*a*
φ_2^v, Z^v	SRK	0.1%	*b*
p	const value	0.03 bar	*c*
T	measurement	0.3 K	*d*
ΔV	measurement	0.2×10^{-6} m^3	*d*
W_1	measurement	0.2×10^{-3} g	*d*
υ_2^L	lit. value	20%	*a*

[a] Estimation based on literature results. [b] Based on comparison of SRK Z values with tabulated literature Z values (*5*), assuming the error in φ_2 is comparable with the error in Z^v. [c] A constant value of 1.013 bar was assumed. Atmospheric pressure differences normally vary ±0.03 bar. [d] Estimation is based on the type of measurement used.

Table V. Error Sources for the HTHp Experiments

param	origin	corresponding error	remarks
y_1	SRK	20%	*a*
φ_2^v, Z^v	SRK: CO	0.5%	*b*
	CO_2	1%	*b*
	H_2	0.2%	*b*
	CH_3OH	1%	*b*
	H_2O	1.5%	*b*
p	measurement	0.2 bar	*c*
p_a	measurement	0.1 bar	*c*
p_b	measurement	0.1 bar	*c*
T	measurement	0.3 K	*c*
T_a	measurement	0.3 K	*c*
T_b	measurement	0.3 K	*c*
Z_a	lit. value	0.1%	*d*
Z_b	lit. value	0.1%	*d*
V_{bomb}	measurement	10^{-6} m^3	*c*
ρ_1	measurement	0.5%	*c*
W_1	measurement	0.02 g	*c*
V_{sc}	measurement	10^{-6} m^3	*c*
W_2	measurement	0.2×10^{-3} g	*c*
υ_2^L	lit. value	20%	*a*

[a] Estimation based on literature results. [b] Based on comparison of SRK Z values with tabulated literature Z values (*5*) and Z values calculated with the virial equation of state using literature virial coefficients (*12*), assuming the error in φ_2 is comparable with the error in Z^v. [c] Estimation is based on the type of measurement used. [d] An error of 0.1% is estimated to cover the effects of interpolation inaccuracy of the tabulated literature Z values and the experimental inaccuracies.

Table VI. Contribution of the Errors of the Different Quantities on the Average, ϵ_{av}, and Maximum, ϵ_{max}, Experimental Errors (Equations 14 and 15) of the Pseudoexperimental Henry Constants *H*

	resulting error in H/%			
param	LTLp[a]	LTLp[b]	HTHp[c]	HTHp[d]
y_1	0	0	0	0.73
φ_2^v, Z^v	0.20	0.20	0.59	0.99
p	0.03	0	2.63	1.75
T	0.10	0.09	0.16	0.02
p_a			2.74	
p_b			2.91	
T_a			0.95	
T_b			0.61	
Z_a			0.93	
Z_b			0.60	
ΔV	1.55	6.52		
W_1	0	0	0.03	0
V_{bomb}			1.37	0.29
ρ_1			2.40	0.58
V_{sc}			0.88	
W_2				0.01
υ_2^L	0.04	0.02	0.41	0.10
ϵ_{max}	1.9	6.8	17.2	4.5
ϵ_{av}	1.6	6.5	5.9	2.2

[a] CO_2–$C_{16}H_{34}$, 298.2 K, 1.013 bar. [b] H_2–$C_{13}H_{10}O$, 353.2 K, 1.013 bar. [c] CO–$C_{30}H_{62}$, 421.8 K, 24.9 bar. [d] H_2O–$C_{30}H_{62}$, 563.8 K, 15.4 bar.

elevated pressure (see, e.g., ref 4). The calculation framework yields a pseudoexperimental Henry constant by iteratively minimizing the difference between the real volume of the bomb and the calculated value (eq 12) toward zero.

Experimental Errors. This section describes the various error sources and their effects on the pseudoexperimental Henry constants. Table IV shows the error sources for the LTLp experiments while Table V deals with the HTHp experiments.

The applicability of SRK to calculate Z^V values (for pure solute) was examined by comparing SRK results with tabulated Z^V values (*5*) or with Z^V values calculated with the use of the virial equation of state and literature virial coefficients (*12*). These literature virial coefficients have been derived from experimental results. Therefore, Z^V values calculated with this method may be regarded as "experimental" values. It is further assumed that the relative error of φ_2^V is equal to that of Z^V and that the presence of the solvent in the vapor phase does not influence the estimated relative errors. These assumptions are reasonable since the mole fractions of the solvents in the vapor phase were always very small (calculated y_1 values fall in the range 0–0.04).

The applicability of SRK to calculate y_1 values was examined by comparing SRK results with literature values (*13*). For the system CO_2–hexadecane (T = 461.7 and 542.3 K; 20–100 bar) an average error of 13% is found. It is concluded that an overall error of 20% for y_1 seems a reasonable (rather pessimistic) estimation.

The assumed error of 20% for v_2^L is in fact an overall error to cover deviations from volume additivity and the influences of solvent on v_2^L. The error value was estimated from various v_2^L values reported by Reid et al. (*4*).

The overall effect of the error sources on the pseudoexperimental Henry constants is calculated as follows.

$$\epsilon_{max} = 100\sum_{i=1}^{N}\left(\left|\frac{\partial H}{\partial \alpha_i}\right|\frac{\Delta\alpha_i}{H_{exptl}}\right) \qquad (14)$$

$$\epsilon_{av} = 100\left[\sum_{i=1}^{N}\left(\frac{\partial H}{\partial \alpha_i}\,\frac{\Delta\alpha_i}{H_{exptl}}\right)^2\right]^{1/2} \qquad (15)$$

In these equations α_i and $\Delta\alpha_i$ symbolize the various quantities contributing to the overall error and the corresponding absolute error coupled to these quantities, respectively. The partial derivatives $\partial H/\partial \alpha_i$ were calculated numerically.

Table VI showed the detailed results of the error calculations of some experiments. All estimated overall errors are listed in Table VII together with the experimental results and the pseudoexperimental Henry constants. As can be seen from Table VI the most significant error source for the LTLp experiments is the measuring accuracy of ΔV. For the HTHp experiments no single predominant error source exists. Therefore, the overall average error is much lower than the overall maximum error, since it is unlikely that all error sources would lead to contributions in the same direction. The influence of the models (SRK and the volume additivity assumption) is rather small, which means that the experimental inaccuracies predominate.

Comparison with Literature Results. In Table VIII the Henry constants obtained in this study are compared with those from the literature. A complicating factor in this comparison is the fact that the literature results were not always obtained at the same pressures and temperatures as employed in this study. Therefore, SRK (*6*) (with optimal binary interaction coefficients from Table XVI; see later in this paper) was used to correct the experimental results to the pressure and tem-

Table VII. Solubilities of CO, CO_2, H_2, CH_3OH, and H_2O in Hexadecane, Squalane, Octadecane, and Benzophenone at Several Pressures p and Temperatures T

LTLp Experiments (p = 1.013 bar)

run	T/K	ΔV/mL	H/bar	ϵ_{max}/%	ϵ_{av}/%	W_1/g	run	T/K	ΔV/mL	H/bar	ϵ_{max}/%	ϵ_{av}/%	W_1/g
Solute, CO; Solvent, Hexadecane													
1	298.2	7.731	567.0	2.8	2.5	40.0353	5	333.2	9.132	536.7	2.5	2.2	
2	303.2	7.982	558.5	2.8	2.5		6	343.2	9.549	528.7	2.4	2.1	
3	313.2	8.271	556.9	2.7	2.4		7	353.2	10.034	517.8	2.3	2.0	
4	323.2	8.901	534.1	2.5	2.2								
Solute, CO_2; Solvent, Hexadecane													
8	298.2	12.557	74.3	1.9	1.6	8.5084	12	333.2	10.766	96.8	2.2	1.8	
9	303.2	12.478	76.0	1.9	1.6		13	343.2	10.133	105.9	2.3	1.9	
10	313.2	11.688	83.8	2.0	1.7		14	353.2	9.584	115.2	2.4	2.0	
11	323.2	11.181	90.4	2.1	1.8								
Solute, H_2; Solvent, Hexadecane													
15	293.2	2.316	1330.8	8.3	7.9	28.6203	19	333.2	3.577	979.5	5.6	5.3	
16	303.2	2.641	1207.0	7.4	7.0		20	343.2	3.904	924.4	5.2	4.9	
17	313.2	2.908	1132.4	6.8	6.4		21	353.2	4.113	902.8	4.9	4.6	
18	323.2	3.252	1045.0	6.1	5.8								
Solute, CO; Solvent, Octadecane													
22	303.2	6.713	527.7	3.2	2.9	35.7544	26	333.2	7.723	504.4	2.8	2.5	
23	313.2	6.894	530.9	3.1	2.8		27	343.2	7.985	502.6	2.8	2.4	
24	318.2	7.338	506.9	3.0	2.7		28	353.2	8.322	496.3	2.7	2.4	
25	323.2	7.510	503.1	2.9	2.6								
Solute, CO_2; Solvent, Octadecane													
29	303.2	14.238	72.7	1.7	1.4	10.4338	34	328.2	12.180	92.0	2.0	1.6	
30	308.2	13.191	79.8	1.8	1.5		35	333.2	11.565	98.3	2.0	1.7	
31	313.2	13.331	80.2	1.8	1.5		36	343.2	11.203	104.6	2.1	1.8	
32	318.2	13.102	82.9	1.9	1.5		37	353.2	11.192	107.8	2.1	1.8	
33	323.2	12.717	86.8	1.9	1.5								
Solute, H_2; Solvent, Octadecane													
38	303.2	2.669	1215.3	7.3	7.0	32.7311	41	333.2	3.272	1028.5	6.1	5.8	30.8945
39	313.2	2.948	1136.7	6.7	6.4	32.7311	42	343.2	3.822	960.9	5.3	5.0	32.7311
40	323.2	3.052	1069.5	6.5	6.1	30.8945	43	353.2	4.089	924.3	5.0	4.7	32.7311
Solute, CO; Solvent, Squalane													
44	295.6	5.176	345.8	4.0	3.7	30.7557	49	318.0	4.035	336.3	5.0	4.7	21.6636
45	301.0	3.753	342.1	5.4	5.0	21.6636	50	323.2	4.015	343.5	5.1	4.7	21.6636
46	304.2	3.835	338.4	5.3	4.9	21.6636	51	333.2	4.102	346.7	5.0	4.6	21.6636
47	305.1	3.742	347.8	5.4	5.1	21.6636	52	343.6	4.242	345.7	4.8	4.5	21.6636
48	313.2	5.339	355.3	3.9	3.6	30.7557	53	351.4	4.269	351.4	4.8	4.5	21.6636
Solute, CO_2; Solvent, Squalane													
54	295.8	14.841	41.6	1.7	1.3	10.4874	60	322.9	12.033	55.8	2.0	1.6	
55	301.0	14.501	43.3	1.7	1.3		61	328.9	11.906	57.4	2.0	1.6	
56	305.3	13.976	45.5	1.8	1.4		62	335.3	11.259	61.9	2.1	1.7	
57	309.0	13.307	48.4	1.8	1.5		63	343.8	10.952	65.2	2.1	1.8	
58	315.2	12.753	51.4	1.9	1.5		64	353.2	10.392	70.6	2.2	1.9	
59	319.4	12.520	53.1	1.9	1.6								
Solute, H_2; Solvent, Squalane													
65	293.3	3.024	808.5	6.5	6.2	42.3560	69	333.2	4.011	692.7	5.1	4.7	42.3560
66	304.0	3.188	787.9	6.2	5.9	41.9828	70	342.7	4.289	666.3	4.8	4.5	42.3560
67	313.2	3.428	755.0	5.8	5.5	41.9828	71	352.9	4.662	631.3	4.4	4.1	42.3560
68	323.3	3.849	700.4	5.2	4.9	42.3560							
Solute, CO; Solvent, Benzophenone													
72	323.2	2.253	1960.8	8.5	8.2	29.9789	74	343.2	2.539	1848.0	7.6	7.3	
73	333.2	2.435	1870.7	7.9	7.6		75	353.2	2.581	1870.8	7.5	7.2	
Solute, CO_2; Solvent, Benzophenone													
76	323.2	12.835	143.1	1.9	1.5	12.4860	79	343.2	11.381	171.4	2.1	1.7	
77	328.2	12.554	148.5	1.9	1.6		80	353.2	10.214	196.5	2.2	1.9	
78	333.2	12.678	149.4	1.9	1.6								
Solute, H_2; Solvent, Benzophenone													
81	323.2	2.104	4424.9	9.0	8.7	63.1377	84	348.2	2.755	3640.3	7.1	6.8	
82	333.2	2.407	3987.5	8.0	7.7		85	353.2	2.865	3550.5	6.8	6.5	
83	343.2	2.703	3657.3	7.2	6.9								

HTHp Experiments (V_{bomb} = 508.0 mL; V_{sc} = 353.8 mL)

run	p/bar	T/K	H/bar	ϵ_{max}/%	ϵ_{av}/%	W_1/g	run	p/bar	T/K	H/bar	ϵ_{max}/%	ϵ_{av}/%	W_1/g
Solute, CO; Solvent, Octadecane[a]													
86	30.8	432.1	513.9	16.0	5.3	235.31	89	32.3	462.7	456.2	13.1	4.3	
87	31.2	442.2	487.8	14.8	4.9		90	32.8	473.0	440.8	12.3	4.0	
88	31.7	452.8	467.7	13.8	4.5		91	33.4	483.5	429.5	11.6	3.8	

Table VII (Continued)

HTHp Experiments (V_{bomb} = 508.0 mL; V_{sc} = 353.8 mL)

run	p/bar	T/K	H/bar	ϵ_{max}/%	ϵ_{av}/%	W_1/g	run	p/bar	T/K	H/bar	ϵ_{max}/%	ϵ_{av}/%	W_1/g
						Solute, CO; Solvent, Octadecane[a]							
92	34.0	493.3	420.7	11.1	3.7		96	36.6	534.6	388.7	9.4	3.1	
93	34.8	503.6	416.5	10.7	3.5		97	37.2	545.0	380.0	9.1	3.0	
94	35.4	514.2	406.2	10.2	3.4		98	37.8	555.1	371.9	8.9	2.9	
95	36.0	524.3	397.6	9.8	3.2		99	38.6	565.7	366.5	8.7	2.8	
						Solute, CO_2; Solvent, Octadecane[b]							
100	19.5	421.7	141.4	7.6	2.6	235.31	108	25.1	504.2	171.1	7.1	2.3	
101	20.0	432.2	143.5	7.4	2.5		109	25.8	514.2	173.9	7.1	2.2	
102	20.8	442.4	148.9	7.4	2.5		110	26.4	524.7	175.2	7.0	2.2	
103	21.5	452.8	152.9	7.3	2.4		111	27.3	534.7	179.3	7.1	2.2	
104	22.3	463.2	157.8	7.3	2.4		112	28.1	545.2	181.8	7.1	2.2	
105	22.9	473.5	160.4	7.2	2.4		113	28.9	552.4	184.1	7.2	2.2	
106	23.7	483.8	164.9	7.2	2.3		114	30.0	565.7	188.5	7.3	2.2	
107	24.3	493.7	167.2	7.1	2.3								
						Solute, H_2; Solvent, Octadecane[c]							
115	51.2	442.3	808.1	18.7	6.1	235.31	122	58.0	514.5	576.7	11.0	3.6	
116	52.0	452.8	748.0	16.8	5.5		123	59.1	524.9	559.1	10.4	3.4	
117	52.7	463.0	696.3	15.2	5.0		124	60.4	535.0	547.9	10.0	3.3	
118	53.5	473.3	656.7	13.9	4.6		125	61.6	545.3	534.1	9.5	3.1	
119	54.6	483.7	632.8	13.0	4.3		126	62.8	555.3	521.7	9.1	3.0	
120	55.5	493.6	607.3	12.2	4.0		127	64.1	565.7	510.1	8.8	2.9	
121	56.7	503.9	591.0	11.6	3.8								
						Solute, CO; Solvent, Squalane[d]							
128	24.9	421.8	329.0	17.2	5.9	250.32	136	31.0	503.7	323.3	12.8	4.4	
129	25.5	431.9	324.0	16.4	5.6		137	31.8	513.9	321.8	12.3	4.2	
130	26.3	442.3	325.8	15.8	5.4		138	32.5	524.1	317.6	11.8	4.0	
131	27.2	452.9	329.8	15.4	5.2		139	33.2	534.3	313.3	11.3	3.9	
132	27.9	462.9	327.8	14.8	5.0		140	33.9	544.5	308.9	10.9	3.7	
133	28.7	473.2	327.9	14.3	4.9		141	34.7	554.7	306.3	10.5	3.6	
134	29.5	483.5	327.4	13.8	4.7		142	35.4	564.5	302.2	10.2	3.5	
135	30.3	493.4	327.3	13.3	4.5								
						Solute, CO_2; Solvent, Squalane[e]							
143	24.8	421.9	105.3	6.6	2.1	250.32	151	34.5	503.8	145.1	6.5	2.0	
144	26.1	431.9	111.4	6.7	2.1		152	35.6	514.1	148.6	6.5	2.0	
145	27.4	442.3	117.3	6.7	2.1		153	36.7	524.4	151.8	6.5	2.0	
146	28.6	452.9	122.4	6.6	2.1		154	37.7	534.5	154.2	6.4	2.0	
147	29.8	462.9	127.5	6.6	2.1		155	38.9	544.9	157.6	6.4	1.9	
148	31.0	473.2	132.3	6.6	2.1		156	40.0	555.1	160.1	6.4	1.9	
149	32.1	483.5	136.3	6.6	2.0		157	41.0	565.1	162.0	6.4	1.9	
150	33.2	493.5	140.2	6.5	2.0								
						Solute, H_2; Solvent, Squalane[f]							
158	76.6	421.9	574.9	16.7	5.5	250.32	161	82.6	452.8	530.0	13.6	4.5	
159	78.5	432.1	556.5	15.5	5.1		162	84.5	462.9	516.4	12.8	4.2	
160	80.5	442.3	542.5	14.6	4.8		163	86.4	472.9	504.3	12.0	4.0	
						Solute, H_2; Solvent, Squalane[g]							
164	69.6	483.6	461.6	12.0	4.0	250.32	169	77.2	533.7	418.3	9.2	3.1	
165	71.1	493.5	452.1	11.3	3.8		170	78.8	543.9	411.7	8.8	2.9	
166	72.7	503.5	444.5	10.8	3.6		171	80.2	553.9	403.3	8.4	2.8	
167	74.2	513.8	434.6	10.2	3.4		172	81.1	564.1	390.2	7.9	2.6	
168	75.7	523.7	426.6	9.7	3.2								
						Solute, CH_3OH; Solvent, Squalane							
173	9.5	453.1	32.6	3.7	2.5	253.16	179	15.6	513.8	54.7	3.2	1.8	
174	10.5	462.8	36.2	3.5	2.3	(W_2 = 8.4391)	180	16.5	523.9	57.9	3.2	1.7	
175	11.6	473.2	40.2	3.4	2.2		181	17.4	533.9	60.9	3.2	1.7	
176	12.7	483.4	44.2	3.3	2.0		182	18.3	544.3	63.9	3.3	1.6	
177	13.6	493.4	47.5	3.2	1.9		183	19.3	554.3	67.2	3.4	1.6	
178	14.5	503.5	50.7	3.2	1.9		184	20.2	564.5	69.9	3.5	1.7	
						Solute, H_2O; Solvent, Squalane							
185	10.1	462.4	66.9	4.5	2.9	249.65	191	13.4	523.4	88.5	4.2	2.4	
186	10.7	472.8	71.2	4.4	2.8	(W_2 = 2.5418)	192	14.0	533.7	92.0	4.2	2.3	
187	11.3	483.1	75.4	4.3	2.7		193	14.5	543.7	94.5	4.3	2.3	
188	11.9	493.1	79.6	4.3	2.6		194	14.9	553.5	96.0	4.4	2.2	
189	12.4	503.5	82.7	4.2	2.5		195	15.4	563.8	97.9	4.5	2.2	
190	12.9	513.5	85.7	4.2	2.4								
						Solute, CO; Solvent, Benzophenone[h]							
196	31.8	422.0	1617.0	29.4	9.6	310.68	200	35.8	462.9	1572.6	25.1	8.2	
197	32.7	432.1	1588.6	28.0	9.1		201	36.8	473.2	1548.5	24.0	7.8	
198	33.7	442.3	1582.2	26.9	8.8		202	37.7	483.3	1506.4	22.8	7.4	
199	34.8	452.6	1592.9	26.2	8.6		203	38.7	493.6	1477.9	21.8	7.1	

Table VII (Continued)

HTHp Experiments (V_{bomb} = 508.0 mL; V_{sc} = 353.8 mL)

run	p/bar	T/K	H/bar	ϵ_{max}/%	ϵ_{av}/%	W_1/g	run	p/bar	T/K	H/bar	ϵ_{max}/%	ϵ_{av}/%	W_1/g
						Solute, CO; Solvent, Benzophenone[h]							
204	39.7	503.8	1449.0	20.8	6.8		208	43.9	544.4	1338.5	17.9	5.8	
205	40.7	514.0	1417.7	20.0	6.5		209	45.0	555.0	1303.5	17.2	5.5	
206	41.7	524.1	1386.1	19.1	6.2		210	46.1	565.0	1274.5	16.6	5.4	
207	42.8	534.5	1360.2	18.4	6.0								
						Solute, CO_2; Solvent, Benzophenone[i]							
211	19.6	422.0	305.5	8.9	3.2	310.68	219	26.3	503.8	403.7	8.8	3.0	
212	20.4	432.1	318.9	8.9	3.2		220	27.2	513.8	414.5	8.8	2.9	
213	21.3	442.6	334.4	8.9	3.1		221	28.0	524.2	420.8	8.8	2.9	
214	22.2	452.6	350.0	8.9	3.1		222	28.9	534.5	428.9	8.9	2.9	
215	23.0	463.0	361.4	8.9	3.1		223	29.8	544.6	436.0	8.9	2.9	
216	23.8	473.2	372.4	8.8	3.0		224	30.7	555.0	441.3	9.0	2.9	
217	24.6	483.2	382.9	8.8	3.0		225	31.6	565.0	446.0	9.1	2.9	
218	25.5	493.6	395.1	8.8	3.0								
						Solute, H_2; Solvent, Benzophenone[j]							
226	52.1	422.0	2554.1	36.0	11.6	310.68	234	62.8	504.0	1675.1	19.2	6.2	
227	53.5	432.2	2420.4	33.1	10.7		235	64.1	514.4	1598.1	17.9	5.8	
228	54.9	442.4	2299.0	30.5	9.9		236	65.5	524.4	1544.9	17.0	5.5	
229	56.3	452.8	2178.7	28.1	9.1		237	66.8	534.9	1476.1	16.0	5.2	
230	57.8	463.1	2097.9	26.3	8.5		238	68.0	545.3	1406.4	15.0	4.8	
231	59.0	473.2	1962.0	24.0	7.8		239	69.2	555.3	1348.1	14.2	4.6	
232	60.3	483.3	1868.3	22.3	7.2		240	70.5	565.7	1294.7	13.6	4.3	
233	61.6	493.7	1772.1	20.7	6.7								
						Solute, CH_3OH; Solvent, Benzophenone							
241	9.6	462.7	41.9	3.6	2.4	310.68	246	16.5	513.7	72.8	3.2	1.7	
242	10.9	473.1	47.7	3.4	2.2	(W_2 = 16.348)	247	17.9	524.3	79.0	3.2	1.7	
243	12.2	483.2	53.6	3.3	2.0		248	19.8	534.2	87.4	3.3	1.7	
244	13.6	493.3	59.9	3.2	1.9		249	21.4	544.3	94.3	3.4	1.7	
245	15.1	503.8	66.6	3.2	1.8								
						Solute, H_2O; Solvent, Benzophenone							
250	8.6	462.8	32.4	4.2	2.8	310.68	256	20.1	524.1	76.6	3.3	1.8	
251	10.2	473.1	38.5	3.8	2.5	(W_2 = 11.1914)	257	22.2	534.3	84.6	3.3	1.8	
252	12.1	483.3	45.8	3.6	2.3		258	24.5	544.7	93.3	3.4	1.8	
253	13.9	493.6	52.7	3.4	2.1		259	26.7	554.7	101.5	3.5	1.8	
254	15.9	503.7	60.5	3.3	2.0		260	29.1	565.0	110.4	3.7	1.9	
255	17.9	514.1	68.1	3.3	1.9								

[a] From eq 6, p_a = 39.60 bar, T_a = 293.8 K, Z_a = 0.9885, p_b = 26.05 bar, T_b = 294.1 K, Z_b = 0.9914. [b] From eq 6, p_a = 36.50 bar, T_a = 297.2 K, Z_a = 0.7847, p_b = 25.65 bar, T_b = 296.8 K, Z_b = 0.8565. [c] From eq 6, p_a = 57.05 bar, T_a = 295.0 K, Z_a = 1.0336, p_b = 36.05 bar, T_b = 294.2 K, Z_b = 1.0210. [d] From eq 6, p_a = 32.55 bar, T_a = 293.7 K, Z_a = 0.9898, p_b = 21.40 bar, T_b = 293.4 K, Z_b = 0.9925. [e] From eq 6, p_a = 41.45 bar, T_a = 293.8 K, Z_a = 0.7314, p_b = 29.95 bar, T_b = 292.7 K, Z_b = 0.8175. [f] From eq 6, p_a = 91.50 bar, T_a = 294.2 K, Z_a = 1.0549, p_b = 58.30 bar, T_b =293.2 K, Z_b = 1.0344. [g] From eq 6, p_a = 71.95 bar, T_a = 291.6 K, Z_a = 1.0429, p_b = 46.20 bar, T_b = 290.9 K, Z_b = 1.0272. [h] From eq 6, p_a = 36.97 bar, T_a = 293.2 K, Z_a = 0.9887, p_b = 22.51 bar, T_b = 293.2 K, Z_b = 0.9922. [i] From eq 6, p_a = 31.40 bar, T_a = 295.4 K, Z_a = 0.8150, p_b = 20.30 bar, T_b = 295.4 K, Z_b = 0.8870. [j] From eq 6, p_a = 61.45 bar, T_a = 296.0 K, Z_a = 1.0362, p_b = 37.25 bar, T_b = 295.0 K, Z_b = 1.0217.

Table VIII. Comparison of the Henry Constants Obtained in This Study with Those in the Literature

ref	system	exptl conditions (lit. results)		mean[b] deviation/%
		p/bar	T/K	
14	H_2-$C_{30}H_{62}$	1.013	300–375	4
15	CO-$C_{16}H_{34}$	1.013	300–375	2
15	CO_2-$C_{16}H_{34}$	1.013	300–375	1
3	H_2-$C_{16}H_{34}$	1.013	298–375	4
16	CO_2-$C_{16}H_{34}$	1.013	298–343	2
17	CO_2-$C_{16}H_{34}$	1.013	299–330	1
17	CO_2-$C_{30}H_{62}$	1.013	299–330	6
18	H_2-paraf[a]	10–950	379, 473	7

[a] Compared with octadecane, based on the molecular weight of the paraffin. [b] Defined as

$$\frac{100}{N}\sum_{k=1}^{N}\left|\frac{H_{lit.,k} - H_{exptl,k}}{H_{exptl,k}}\right|$$

perature corresponding to the relevant literature results. These SRK corrections were used for interpolation purposes only; literature results lying outside the experimental temperature ranges were not included in the comparison. In addition, the comparison between literature Henry constants and our experimental results is always based on the nearest values with respect to temperature.

As can be seen from Table VIII, our results agree quite well with those taken from the literature. In most cases the deviations between our results and those taken from the literature are smaller than the estimated maximum experimental errors of our results.

Furthermore, Table VIII shows the experimental conditions corresponding to the literature results. Comparing the literature data with our own results on this point (see Table I), it is clear that the present study gives a large amount of new solubility data. Only our hexadecane results do not provide new information. It should be noted that the choice of this solvent was partly intended to properly check our experimental results with literature data.

The results are also presented in Figures 2 and 3, clearly showing the reasonable degree of agreement. Here, it should be noted that the HTHp results were recalculated to 1.013 bar (again with the use of SRK in combination with optimal binary interaction parameters) in order to obtain comparable results.

The results of Peter and Weinert (*18*) were used to show the effect of pressure (see Table IX). As can be seen the Henry

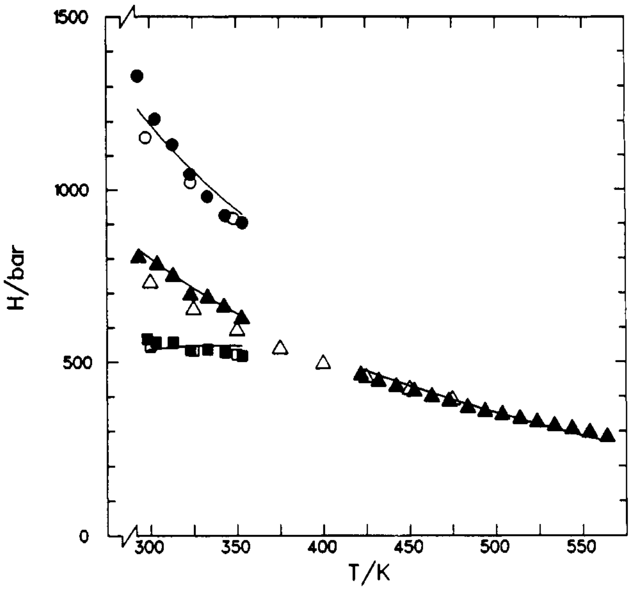

Figure 2. Comparison between experimental and literature Henry constants *H* for CO–hexadecane, H_2–hexadecane, and H_2–squalane (p = 1.013 bar) as a function of temperature *T*: ●, H_2–hexadecane, our results; ○, H_2–hexadecane, Cukor and Prausnitz (*3*); ▲, H_2–squalane, our results; △, H_2–squalane, Chappelow and Prausnitz (*14*); ■, CO–hexadecane, our results; □, CO–hexadecane, Tremper and Prausnitz (*15*); lines, calculated with SRK in combination with the optimal binary interaction parameters given in Table XVI. Note: HTHp results have been corrected to p = 1.013 bar (with SRK).

Table IX. Henry Constants for the System CO_2–Octadecane Obtained by SRK Calculations from the Literature and from This Study

T = 379 K			T = 473 K		
p/bar	$H_{\text{lit.}}{}^{a}$/bar	$H_{\text{lit.}}{}^{a,b,d}$/bar	p/bar	$H_{\text{lit.}}{}^{a}$/bar	$H_{\text{lit.}}{}^{a,b,d}$/bar
9.8	781	766	19.4	578	522
10.0	759	744	21.6	558	530
51.3	855	770	69.2	605[c]	512
95.8	990	814	88.3	665[c]	539
393.4	1518	758	110.4	674	521
			111.3	685	527
		770[c]			
					525[c]

[a] Reference 18. [b] Corrected to p = 1.013 bar with SRK. [c] Average value. [d] Our results: H(379 K) = 814 bar, H(473 K) = 577 bar.

Table X. Models for Predicting Gas–Liquid Solubility As Studied in This Paper

ref	model	abbrevation
6	Soave–Redlich–Kwong equation of state	SRK
19	Peng–Robinson equation of state	PR
20	regular solutions theory	RS
7, 8	group-contribution equation of state	SJGC

constants corrected to a pressure of 1.013 bar are identical for a given temperature within a few percent. This indicates that SRK is able to give a good description of the pressure influence.

Theory

Models for Prediction of Gas–Liquid Solubility. Since it is practically impossible to compare all models and methods available for predicting gas–liquid solubilities, we have restricted this study to four models as presented in Table X.

The familiar equations of state of Soave (*6*) and of Peng and Robinson (*19*) are chosen because they are widely used in engineering practice. In principle, only pure component properties are required for the calculation of gas–liquid solubilities using these equations of state. However, to obtain satisfactory results, binary interaction coefficients are nearly always required.

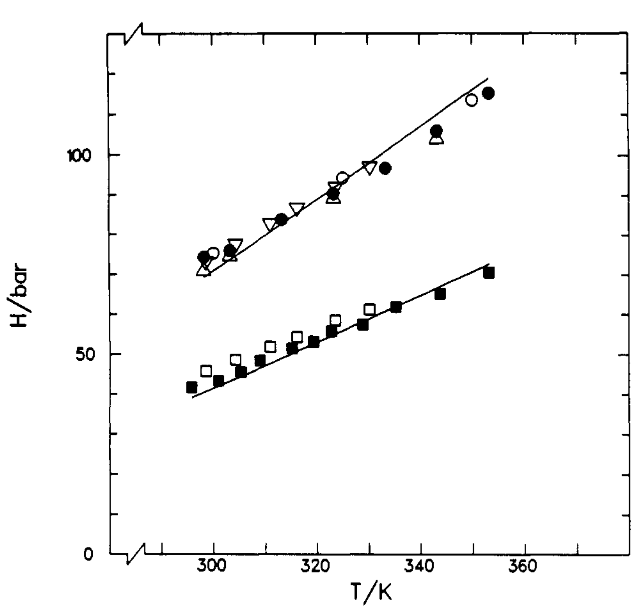

Figure 3. Comparison between experimental and literature Henry constants *H* for CO_2–hexadecane and CO_2–squalane (p = 1.013 bar) as a function of temperature *T*: ●, CO_2–hexadecane, our results; ○, CO_2–hexadecane, Tremper and Prausnitz (*15*); △, CO_2–hexadecane, King and Al Najjar (*16*); ▽, CO_2–hexadecane, Chai and Paulaitis (*17*); ■, CO_2–squalane, our results; □, CO_2–squalane, Chai and Paulaitis (*17*); lines, calculated with SRK in combination with the optimal binary interaction parameters given in Table XVI.

The gas–liquid solubilities are obtained using the following equations (Reid et al. (*4*)).

$$RT \ln f_i^{\mathrm{V}} = \int_{V_{\mathrm{T}}^{\mathrm{V}}}^{\infty} [(\partial p/\partial n_i)_{T,V_{\mathrm{T}},n_j} - RT/V_{\mathrm{T}}] - RT \ln (v^{\mathrm{V}}/y_i RT) \quad (16)$$

$$RT \ln f_i^{\mathrm{L}} = \int_{V_{\mathrm{T}}^{\mathrm{L}}}^{\infty} [(\partial p/\partial n_i)_{T,V_{\mathrm{T}},n_j} - RT/V_{\mathrm{T}}] - RT \ln (v^{\mathrm{L}}/x_i RT) \quad (17)$$

$$f_i^{\mathrm{V}} = f_i^{\mathrm{L}} \quad (18)$$

Equations 16 and 17 are used to calculate the fugacities of component *i* in the vapor and in the liquid phase, respectively. At equilibrium these fugacities are identical, as indicated by eq 18.

According to the regular solutions theory (RS) (*20*), an isothermal solution is reached in two steps: (1) isothermal condensation of the gas into a hypothetical liquid phase and (2) mixing of this hypothetical liquid with the solvent. This leads to the following equation for the Henry constant (*4*):

$$H_{1,2} = f^{\mathrm{L}}_{\mathrm{pure},2} \exp\left[\frac{v_2^{\mathrm{L}}\phi_1^2[(\delta_1 - \delta_2)^2 + 2l_{1,2}\delta_1\delta_2]}{RT}\right] \quad (19)$$

Because of this approach, the fugacity of the hypothetical liquid is required. For subcritical gases or vapors this quantity can be calculated from pure component data. For supercritical gases this quantity is hypothetical and has to be estimated from binary gas–liquid equilibrium data. The binary parameter for RS $l_{1,2}$ is comparable with the binary interaction coefficient $k_{i,j}$ in the Soave–Redlich–Kwong and Peng–Robinson equations of state. For the gas phase the fugacities can be calculated using the Soave–Redlich–Kwong or the Peng–Robinson equation of state (or assuming ideal-gas behavior). The regular solutions theory is selected for investigation because it is probably the

Table XI. Critical Temperatures T_c, Critical Pressures p_c, and Acentric Factors ω of the Compounds

compound	T_c/K	p_c/bar	ω
CO (*4*)	132.9	35.0	0.066
CO_2 (*4*)	304.1	73.8	0.239
H_2 (*4*)	33.0	12.9	−0.216
CH_3OH (*4*)	512.6	80.9	0.556
H_2O (*4*)	647.3	221.2	0.344
hexadecane, $C_{16}H_{34}$ (*4*)	722	14.1	0.742
octadecane, $C_{18}H_{38}$ (*4*)	748	12.0	0.790
squalane, $C_{30}H_{62}$	765 (*24*)	8.6 (*24*)	0.83 (*25*)
benzophenone, $C_{13}H_{10}O$	805 (*24*)	30.4 (*24*)	0.55 (*25*)

Table XII. Solubility Parameters δ and Molar (Liquid) Volumes v^L of the Compounds

compound	$\delta \times 10^{-3}$/ ($J^{1/2}$ $m^{-3/2}$)	$v^L \times 10^6$/ (m^3 mol^{-1})
CO (*26*)	6.40	32.1
CO_2 (*26*)	12.3	55.0
H_2 (*26*)	6.65	31.0
CH_3OH (*26*)	14.5	40.9
H_2O (*26*)	47.9	18.0
hexadecane, $C_{16}H_{34}$	15.2[a]	
octadecane, $C_{18}H_{38}$	14.8[a]	
squalane, $C_{30}H_{62}$	13.5[a]	
benzophenone, $C_{13}H_{10}O$	20.1[a]	

[a] These are the mean values of the results of eqs 22 and 23.

simplest method (with a thermodynamical basis) available for predicting solubilities.

The fourth model we have chosen to investigate is the group-contribution equation of state as presented by Skjold-Jørgensen (*7*, *8*). This method is developed especially for the description of vapor–liquid equilibria at elevated pressures and broad temperature ranges. For this reason it is of particular interest to this study. It is based on the generalized van der Waals partition function (*21*). Skjold-Jørgensen combined the configurational part of the partition function with the excess Helmholtz function, as proposed originally by Mollerup (*22*). The attraction part of the residual Helmholtz function is built up from groups and surface segments in the same way as has been done in the UNIFAC equation (*23*). The free volume part of the residual Helmholtz function is not rewritten in terms of groups: hard sphere diameters of whole molecules are the basis of this contribution. The fugacity coefficients are obtained using eqs 20 and 21 (*7*).

$$\ln \varphi_i = \frac{\partial}{\partial n_i}\left[\frac{A^R}{RT}\right]_{T,V_T,n_{j\neq 1}} - \ln Z \qquad (20)$$

$$Z = -V\frac{\partial}{\partial V_T}\left[\frac{A^C}{RT}\right]_{T,n} \qquad (21)$$

Model Parameters. The most important parameters in the Soave–Redlich–Kwong and the Peng–Robinson equations of state are the critical properties and the acentric factors. The values of these parameters for the compounds investigated in this study are given in Table XI.

The molar (liquid) volumes and the solubility parameters are presented in Table XII. The solubility parameters δ marked with an italic *a* were both calculated from eqs 22 (*4*) and 23 (*27*).

$$\delta = \left[\frac{\Delta U^V}{v}\right]^{1/2} \approx \left[\frac{\Delta H^V - RT}{v}\right]^{1/2} \qquad (22)$$

$$\delta = \sum_i (\Delta Q_i / v) \qquad (23)$$

The reported value of δ is the mean value of the results of these two equations. The hypothetical liquid fugacities of the solutes $f^L_{pure,2}$ as functions of the temperature have been calculated from the following equation (*28*):

$$f^L_{pure,2} = p_c \exp[7.224 - 7.534(T_c/T) - 2.598 \ln (T/T_c)] \qquad (24)$$

Since H_2 has an extremely low critical temperature, eq 24 is not applicable at relatively high temperatures for H_2. Therefore, the results of eq 24 are multiplied with by a factor of 26.95. In this way a good agreement was obtained between calculated hypothetical fugacities and literature values (*29*).

Table XIII. Critical Hard Sphere Diameters d_c

compound	$d_c{}^a \times 10^2$/ (m $mol^{-1/3}$)	$d_c{}^b \times 10^2$/ (m $mol^{-1/3}$)
hexadecane, $C_{16}H_{34}$	7.216	7.245
octadecane, $C_{18}H_{38}$	7.716	7.600
squalane, $C_{30}H_{62}$	8.708	9.500

[a] Equation 25. [b] Vapor pressure.

The critical hard sphere diameters of the solvents d_c are listed in Table XIII. For all solutes d_c was calculated from the critical properties, using eq 25 (*7*). The situation is somewhat more complicated for the solvents, because here the critical properties are not always known with sufficient accuracy. Therefore, d_c was also optimized from pure component data. For hexadecane and octadecane we used the normal boiling points (*4*). For squalane, not even the normal boiling point is known with sufficient accuracy. Therefore, vapor pressure data from the *Merck Index* were used (*30*). These d_c values (marked with the comment "vapor pressure" in Table XIII) were used in the calculations. No d_c values are presented for benzophenone, as will be explained below.

$$d_c = 9.634 \times 10^{-3}(RT_c/p_c)^{1/3} \qquad (25)$$

The necessary parameters for the group-contribution equation of state were taken from ref 8. However, a few necessary parameters are not available. No parameter values are presented by Skjold-Jørgensen (*7*, *8*) for the carbonyl group in benzophenone and for the interaction between aromatic ring groups and water. This means that no calculations with the group-contribution equation of state can be made for the benzophenone-containing systems.

For the parameter optimization the following objective function was used.

$$\text{objective function} = \sum_{k=1}^{N}\left[\frac{H_k^{calc} - H_{exptl,k}}{H_{exptl,k}}\right]^2 \qquad (26)$$

The adjustable parameters are the binary interaction coefficients for the cubic equations of state and the regular solutions theory. For the Skjold-Jørgensen equation of state the values of the critical hard sphere diameters were optimized because the calculated Henry constants are very sensitive to these parameter values. It should be noted that for a total optimization of the parameter base our experimental results should be combined with the experimental data base used by Skjold-Jørgensen (*7*, *8*).

Experimental Henry Constants and Model Calculations

The results of all experiments are given in Figures 4–8 and in Table VII. In these figures, the open symbols are always used for LTLp results and the closed symbols for the HTHp results. From Figures 4–8 it can be seen that the LTLp and the HTHp results for a given binary system are fairly well represented by a single line, which means that deviations from Henry's law due to pressure influences are not very large for

Table XIV. Comparison between Experimental Errors and the Deviations[a] between Calculated and Experimental Values of the Henry Constants for the LTLp Results

	exptl[b] error		RS		SRK		PR		SJGC	
system	av	max	*c*	*d*	*c*	*d*	*c*	*d*	*c*	*d*
CO–$C_{16}H_{34}$	2	3	1	1	16	4	20	4	18	8
CO–$C_{18}H_{38}$	3	3	3	10	20	2	23	4	20	16
CO–$C_{30}H_{62}$	5	5	14	6	17	2	18	3	43	31
CO–$C_{13}H_{10}O$	8	8	4	32	20	3	30	2	*e*	*e*
CO_2–$C_{16}H_{34}$	2	2	9	9	38	3	35	4	6	5
CO_2–$C_{18}H_{38}$	2	2	9	50	37	9	34	11	9	7
CO_2–$C_{30}H_{62}$	2	2	33	44	7	3	3	3	12	4
CO_2–$C_{13}H_{10}O$	2	2	75	6	40	3	42	3	*e*	*e*
H_2–$C_{16}H_{34}$	6	6	29	2	22	4	29	4	26	9
H_2–$C_{18}H_{38}$	6	6	16	23	32	6	37	3	34	30
H_2–$C_{30}H_{62}$	5	5	42	22	30	1	33	2	48	38
H_2–$C_{13}H_{10}O$	7	8	5	32	34	3	45	2	*e*	*e*
total LTLp	4	4	20	20	25	3	27	4	23	16

[a] Deviations are defined as

$$\frac{100}{N}\sum_{k=1}^{N}\left|\frac{H_{\text{exptl}}-H^{\text{calc}}}{H_{\text{exptl}}}\right|_k$$

[b] Including reproducibility and systematic effects. [c] No parameter optimization employed. [d] With optimal parameter values as presented in Tables XVI and XVII. [e] Necessary model parameters are unavailable.

Table XV. Comparison between Experimental Errors and the Deviations[a] between Calculated and Experimental Values of the Henry Constants for the HTHp Results

	exptl[b] error		RS		SRK		PR		SJGC	
system	av	max	*c*	*d*	*c*	*d*	*c*	*d*	*c*	*d*
CO–$C_{18}H_{38}$	4	11	16	9	6	2	4	5	2	5
CO–$C_{30}H_{62}$	5	13	6	8	7	5	5	5	14	1
CO–$C_{13}H_{10}O$	7	22	38	25	13	6	18	4	*e*	*e*
CO_2–$C_{18}H_{38}$	2	7	78	21	5	10	2	12	21	24
CO_2–$C_{30}H_{62}$	2	7	101	23	4	4	5	5	8	19
CO_2–$C_{13}H_{10}O$	3	9	55	4	20	1	21	1	*e*	*e*
H_2–$C_{18}H_{38}$	4	12	34	32	24	7	25	4	7	4
H_2–$C_{30}H_{62}$	4	12	21	29	17	3	18	3	10	6
H_2–$C_{13}H_{10}O$	7	22	44	33	22	2	28	2	*e*	*e*
CH_3OH–$C_{30}H_{62}$	2	3	1147	11	23	3	18	3	9	4
CH_3OH–$C_{13}H_{10}O$	2	3	85	1	33	1	33	1	*e*	*e*
H_2O–$C_{30}H_{62}$	3	4	6740	23	45	4	39	3	7	16
H_2O–$C_{13}H_{10}O$	2	4	1277	3	35	11	31	10	*e*	*e*
total HTHp	4	8	620	18	18	5	18	4	10	10

[a–e] See Table XIV.

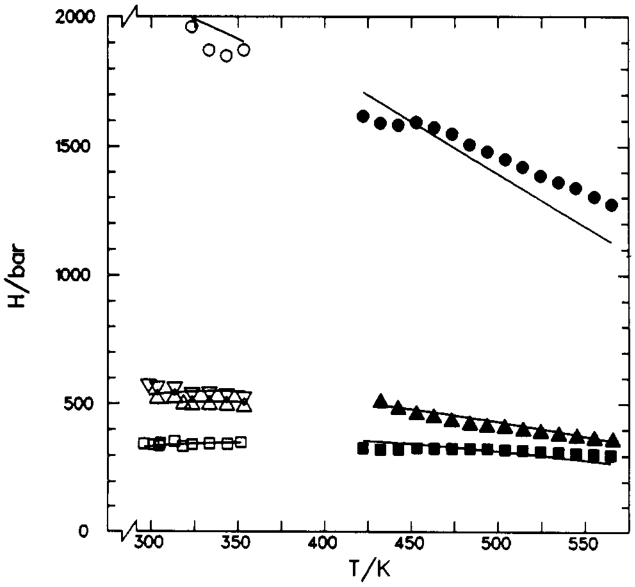

Figure 4. Henry constants *H* of CO in various solvents as a function of temperature *T*: open symbols, LTLp results; closed symbols, HTHp results; ○, ●, benzophenone; □, ■, squalane; △, ▲, octadecane; ▽, hexadecane; lines, calculated with SRK in combination with the optimal binary interaction coefficients given in Table XVI.

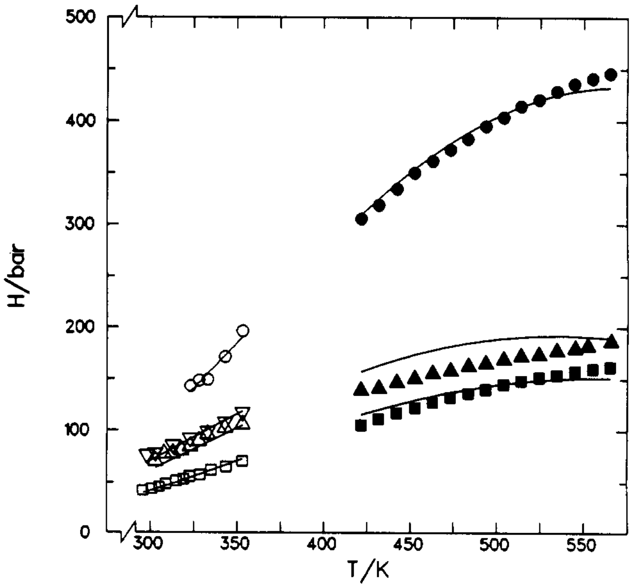

Figure 5. Henry constants *H* of CO_2 in various solvents as a function of temperature *T*: open symbols, LTLp results; closed symbols, HTHp results; ○, ●, benzophenone; □, ■, squalane; △, ▲, octadecane; ▽, hexadecane; lines, calculated with SRK in combination with the optimal binary interaction coefficients given in Table XVI.

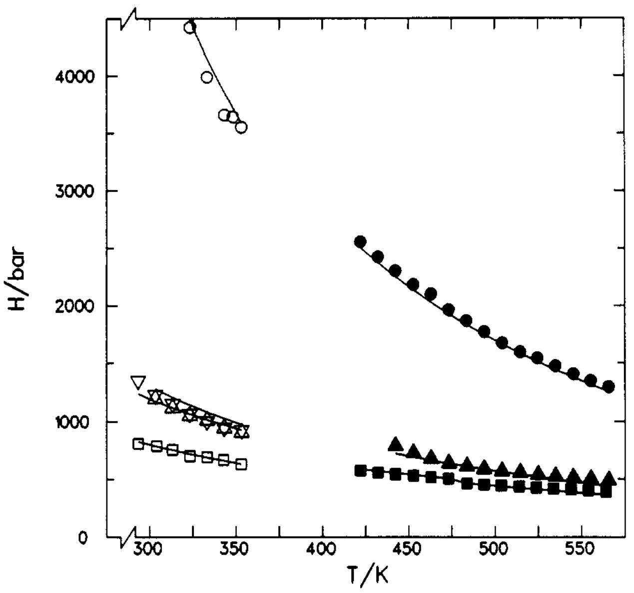

Figure 6. Henry constants *H* of H_2 in various solvents as a function of temperature *T*: open symbols, LTLp results; closed symbols, HTHp results; ○, ●, benzophenone; □, ■, squalane; △, ▲, octadecane; ▽, hexadecane; lines, calculated with SRK in combination with the optimal binar interaction coefficients given in Table XVI.

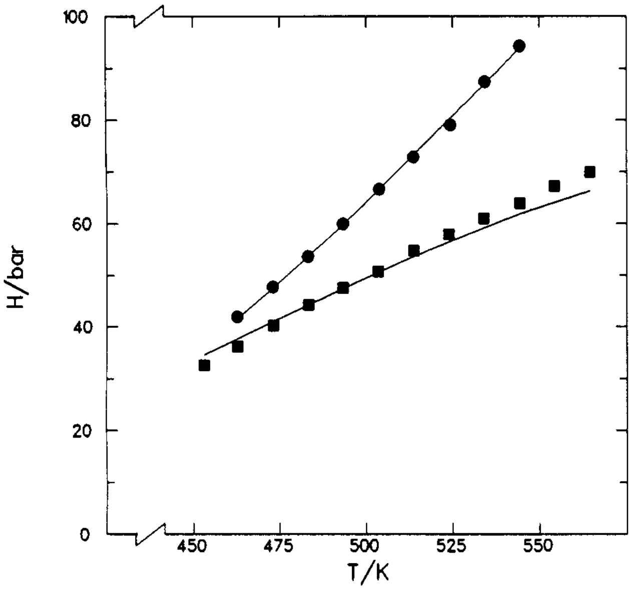

Figure 7. Henry constants *H* of CH_3OH in various solvents as a function of temperature *T*: ●, benzophenone; ■, squalane; lines, calculated with SRK in combination with the optimal binary interaction coefficients given in Table XVI.

these systems under the conditions studied.

In Tables XIV and XV the deviations between experimental solubilities and model predictions are given. For the values in the "*c*" columns no parameter optimization was employed and zero binary interaction coefficients were taken for the Peng–Robinson and Soave–Redlich–Kwong equations of state and the regular solutions theory. The binary interaction coefficients (of groups) for the group-contribution equation of state are taken from Skjold-Jørgensen (*7*, *8*). It can be seen from Table XV that completely erroneous Henry coefficients are calculated for the water- and methanol-containing systems when using the regular solutions theory. Except for these cases, the results of all four models are quite comparable when using zero binary interaction parameters and unoptimized hard sphere diameters, slightly favoring the group-contribution equation of state with an average deviation between the calculated and the experimental Henry constants of 15%.

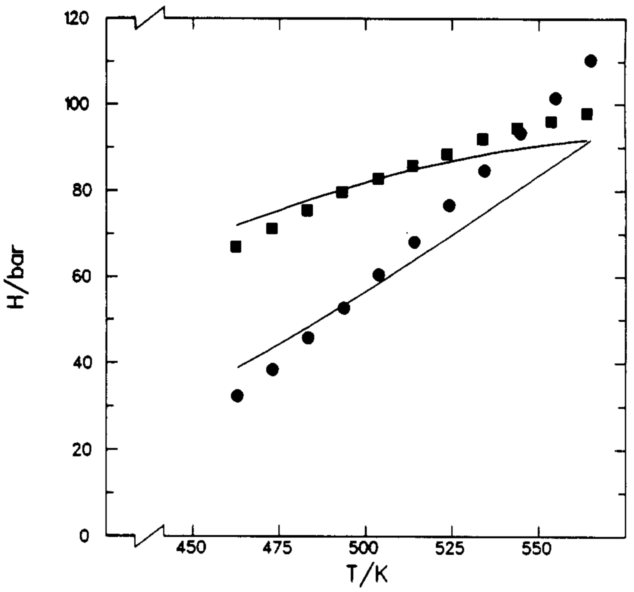

Figure 8. Henry constants *H* of H_2O in various solvents as a function of temperature *T*: ●, benzophenone; ■, squalane; lines, calculated with SRK in combination with the optimal binary interaction coefficients given in Table XVI.

Table XVI. Optimal Values for the Binary Interaction Coefficients

system	$l_{1,2}$(RS)	$k_{i,j}$(SRK)	$k_{i,j}$(PR)
$CO-C_{16}H_{34}$	0.001	0.102	0.115
$CO-C_{18}H_{38}$	0.053	0.136	0.129
$CO-C_{30}H_{62}$	−0.033	0.119	0.104
$CO-C_{13}H_{10}O$	0.098	0.113	0.147
$CO_2-C_{16}H_{34}$	0.008	0.123	0.110
$CO_2-C_{18}H_{38}$	−0.086	0.101	0.079
$CO_2-C_{30}H_{62}$	−0.117	0.018	−0.005
$CO_2-C_{13}H_{10}O$	−0.064	0.097	0.097
$H_2-C_{16}H_{34}$	−0.110	0.335	0.342
$H_2-C_{18}H_{38}$	0.026	0.639	0.535
$H_2-C_{30}H_{62}$	−0.073	0.584	0.471
$H_2-C_{13}H_{10}O$	0.089	0.444	0.439
$CH_3OH-C_{30}H_{62}$	−0.341	0.110	0.082
$CH_3OH-C_{13}H_{10}O$	−0.059	0.101	0.097
$H_2O-C_{30}H_{62}$	−0.796	0.287	0.232
$H_2O-C_{13}H_{10}O$	−0.340	0.115	0.094

Table XVII. Optimal Values for the Critical Hard Sphere Diameters

solvent	$d_c \times 10^2$/ (m mol$^{-1/3}$)
hexadecane, $C_{16}H_{34}$	7.137
octadecane, $C_{18}H_{38}$	7.574
squalane, $C_{30}H_{62}$	9.355

The deviations given in the "*d*" columns are obtained after parameter optimization. The obtained optimal binary interaction coefficients for the Peng–Robinson equation of state, the Soave–Redlich–Kwong equation of state, and the regular solutions theory are given in Table XVI. For the group-contribution equation of state only hard sphere diameters were optimized. The optimal values of the critical hard sphere diameters are given in Table XVII.

As can be seen in Tables XIV and XV the results of the regular solutions theory are reasonable. A very good agreement is obtained with the cubic equations of state, both giving almost the same results.

However, it should be borne in mind that for each binary system one extra parameter is needed, which can only be obtained from experimental data. On the other hand, only a few reliable experimental binary data (in principle only one is sufficient) are needed to obtain the optimal binary interaction coefficient. After this, the cubic equations of state have a good extrapolating power. Fairly good results are obtained using the group-contribution equation of state, especially because only a small number of parameters is optimized. An optimization of the various binary interaction parameters (of groups) was not undertaken because many more data are required for such an approach. However, it is likely that an optimization of these parameters will result in a very good agreement between experimental data and model predictions.

Conclusions

On the basis of an extensive set of experimental solubility data, the following conclusions can be made regarding the models used for predicting the solubilities of the components of the methanol synthesis in various solvents.

Regular Solutions Theory. When using no binary interaction parameters, this theory predicts erroneous Henry coefficients for systems containing water and methanol. For systems containing CO, CO_2, or H_2 (permanent gases) this method gives reasonable results. The regular solutions theory describes all experimental results reasonably when optimal interaction parameters are used.

Cubic Equations of State. The results of both the Soave–Redlich–Kwong and the Peng–Robinson equations of state are reasonable for zero binary interaction coefficients. By using optimal binary interaction coefficients, these equations of state give an excellent description of the solubilities. This leads to the conclusion that the use of the cubic equations of state is preferable when experimental binary data are available.

Group-Contribution Equation of State. Without parameter optimization this equation of state gives the best results, provided that the necessary parameter values are known. This leads to the conclusion that this method is preferable when no experimental data are available. Optimization of the critical hard sphere diameters of the solvents results in a fairly good agreement with the experimental results.

Our results agree with literature data as far as available. In most cases the deviations between our results and the literature data are smaller than our estimated maximum experimental errors.

Glossary

a	constant in eq 1, kg m^{-3}
A	Helmholtz energy, J mol^{-1}
b	constant in eq 1, kg m^{-3} K^{-1}
d	hard sphere diameter, m $mol^{-1/3}$
f	fugacity, bar
H	Henry constant, bar
$k_{i,j}$	binary interaction coefficient for SRK and PR
$l_{1,2}$	binary parameter for RS
M	molecular weight, g mol^{-1}
n	number of moles, mol
N	number of experiments or of error contributions
p	pressure, bar
R	gas constant (8.314), J mol^{-1} K^{-1}
T	temperature, K
v	molar volume, m^3 mol^{-1}
V_T	total volume, m^3
W	mass of compound, g
x	mole fraction in the liquid phase
y	mole fraction in the vapor phase
Z	compressibility factor
α	auxiliary quantity in error eqs 14 and 15
δ	solubility parameter, $J^{1/2}$ $m^{-3/2}$
Δ	error value
ΔQ	molar attraction constant, $J^{1/2}$ $m^{3/2}$ mol^{-1}
ΔH	enthalpy change, J mol^{-1}
ΔU	energy change, J mol^{-1}
ΔV	volume change, m^3
ϵ	relative error
ρ	density, kg m^{-3}
φ	fugacity coefficient
ϕ	volume fraction
ω	acentric factor

Superscripts

C	configurational
calc	calculated value
L	liquid phase
R	residual
V	vapor phase

Subscripts

a	initial conditions
av	average value
b	final conditions
bomb	of the bomb
c	at the critical point
eff	effective value
exptl	experimental value
i,*j*	component
k	experiment
max	maximum value
pure	for the pure compound
sc	of the supply cylinder
1	solvent
2	solute

Abbreviations

eq	equation
LTLp	low-temperature, low-pressure experiments
HTHp	high-temperature, high-pressure experiments
PR	Peng–Robinson equation of state
RS	regular solutions theory
SJGC	Skjold-Jørgensen group-contribution equation of state
SRK	Soave–Redlich–Kwong equation of state

Registry No. CO, 630-08-0; CO_2, 124-38-9; H_2, 1333-74-0; CH_3OH, 67-56-1; H_2O, 7732-18-5; hexadecane, 544-76-3; octadecane, 593-45-3; squalane, 111-01-3; benzophenone, 119-61-9.

Literature Cited

(1) Meuldijk, J.; Joosten, G. E. H.; Stamhuis, E. J. *J. Mol. Catal.* **1986**, *37*, 75.
(2) Olsen, J. D. *J. Chem. Eng. Data* **1977**, *22*, 326.
(3) Cukor, P. M.; Prausnitz, J. M. *J. Phys. Chem.* **1972**, *76*, 598.
(4) Reid, R. C.; Prausnitz, J. M.; Poling, B. E. *The properties of gases and liquids*, 4th ed.; McGraw-Hill: New York, 1987.
(5) "Gas Encyclopaedia"; L'air liquide. Elsevier: Amsterdam, 1976.
(6) Soave, G. *Chem. Eng. Sci.* **1972**, *27*, 1197.
(7) Skjold-Jørgensen, S. *Fluid Phase Equilib.* **1984**, *16*, 317.
(8) Skjold-Jørgensen, S. *Ind. Eng. Chem. Res.* **1988**, *27*, 110.
(9) Schoemaker, D. P.; Garland, C. W. *Experiments in physical chemistry*, 1st ed.; McGraw-Hill: New York, 1962; pp 430, 431.
(10) Weast, R. C., Ed. *Handbook of Chemistry and Physics*, 58th ed.; CRC Press: Cleveland, OH, 1977.
(11) Mantell, C. L. *Engineering materials handbook*, 1st ed.; McGraw-Hill: New York, 1958; Chapter 5, p 12.
(12) Dymond, J. H.; Smith, E. B. *The virial coefficients of pure gases and mixtures – a critical compilation*; Clarendon Press: Oxford, 1980.
(13) Lin, H.-M.; Sebastian, H. M.; Chao, K.-C. *J. Chem. Eng. Data* **1980**, *25*, 252.
(14) Chappelow, C. C., III; Prausnitz, J. M. *AIChE J.* **1974**, *20*, 1097.
(15) Tremper, K. K.; Prausnitz, J. M. *J. Chem. Eng. Data* **1976**, *21*, 295.
(16) King, M. B.; Al-Najjar, H. *Chem. Eng. Sci.* **1977**, *32*, 1241.
(17) Chai, C.-P.; Paulaitis, M. E. *J. Chem. Eng. Data* **1981**, *26*, 277.
(18) Peter, S.; Weinert, M. *Z. Phys. Chem. N.F.* **1955**, *5*, 114.
(19) Peng, D.; Robinson, D. B. *Ind. Eng. Chem. Fundam.* **1976**, *15*, 59.
(20) Hildebrand, J. H.; Scott, R. L. *Regular Solutions*; Prentice-Hall: Englewood Cliffs, NJ, 1962.
(21) Vera, J. H.; Prausnitz, J. M. *Chem. Eng. J.* **1972**, *3*, 1.
(22) Mollerup, J. *Fluid Phase Equilib.* **1981**, *7*, 121.
(23) Fredeslund, A.; Gmeling, J.; Rasmussen, P. *Vapour-liquid equilibria using UNIFAC, a group contribution method*; Elsevier: Amsterdam, Oxford, New York, 1977.

(24) Lydersen, A. L. Estimation of critical properties of organic compounds. Experimental Station Report 3; University of Wisconsin College of Engineering: Madison, WI, 1955.
(25) Lee, B. I.; Kesler, M. G. *AIChE J.* **1975**, *21*, 510.
(26) Shinoda, K. *Principles of solution and solubility*; Marcel Dekker: New York and Basel, 1978.
(27) Small, P. A. *J. Appl. Chem.* (*London*) **1953**, *3*, 71.
(28) Prausnitz, J. M.; Andersen, T. F.; Grens, E. A.; Eckert, C. A.; Hsieh, R.; O'Connel, J. P. *Computer calculations for multicomponent vapour-liquid and liquid-liquid equilibria*; Prentice-Hall: Englewood Cliffs, NJ, 1980.
(29) Prausnitz, J. M.; Shair, F. H. *AIChE J.* **1961**, *7*, 682.
(30) Windholz, M., Ed. *The Merck Index*, 10th ed.; Merck & Co., Inc.: Rahway, NJ, 1983.

Received for review March 21, 1991. Revised October 7, 1991. Accepted December 30, 1991.

Density, Viscosity, and Refractivity Data of Solutions of Potassium Iodide in *N*-Formylmorpholine–Water at 25, 35, and 45 °C

Souad F. Al-Azzawi* and Etimad I. Allos

Petroleum Research Centre, Jadiriyah, P.O. Box 10039, Baghdad, Iraq

The densities, viscosities, and refractive indexes of a wide range of potassium iodide concentrations in *N*-formylmorpholine–water mixtures have been determined at 25, 35, and 45 °C. From these experimental data, the apparent molar volumes, apparent molar refractivities, and Jones–Dole *B* coefficients have been calculated. It was found that in the investigated range of concentrations the values of the apparent molar volumes and apparent molar refractivities are practically independent of temperature but concentration-dependent. Jones–Dole *B* coefficients show a negative deviation from ideality. The values of *B* are negative for the very low concentrations and positive for the higher concentrations.

Introduction

N-Formylmorpholine (NFM) is a highly polar and dense solvent, showing a good suitability for the recovery of monocyclic aromatic hydrocarbons from petroleum products such as gasoline and reformate (*1*, *2*). Recently the aqueous solutions of NFM have been used on an industrial scale for extraction processes (*3*). The addition of small quantities of water increases the efficiency of NFM for the extraction. The thermodynamic properties of NFM and the aqueous solutions have been studied extensively, and we could not trace in the literature the effect of electrolytes on NFM and NFM-water properties; therefore we have initiated a program to study these effects. In a previous work, we have studied the viscosity behavior of potassium iodide (KI) in NFM solutions at several temperatures (*4*). As a continuation of these studies, we measured here the densities, viscosities, and refractive indexes at 25, 35, and 45 °C of KI solutions in NFM–water mixtures. The obtained results of dilute electrolyte solutions were analyzed in terms of the Jones–Dole equation and the apparent molar volumes and molar refractivities.

Experimental Section

Materials. *N*-Formylmorpholine (NFM), puriss grade (Fluka AG), was used without further purification and kept over an activated molecular sieve of type 4A (Union Carbide) for 2 days before use. The purity was confirmed by GLC analysis and was found to be >99.5 mol %. Potassium iodide (KI), Chemically Pure (Riedel-de Haen AG), was dried for 24 h at 110 °C prior to use and stored over P_2O_5 in a glass desicator.

Density Measurements. Densities were determined with an Anton Paar digital densimeter (DMA 60/602), thermostated to ±0.01 °C. The overall precision of the densities is found to be better than $\pm 2 \times 10^{-5}$ g cm^{-3}.

Viscosity Measurements. Viscosities were determined with a suspended-level Ubbelhode viscometer. The flow times were determined electronically with an electronic timer (Schott-Gerate AVS 400) of precision ±0.01 s, and the temperature of the bath was controlled better than ±0.01 °C. The viscosities of the samples were measured with a reproducibility of ±0.002.

Refractive Index Measurements. Refractive indexes were measured with an Abbe refractometer with a temperature-controlled bath to ±0.01 °C. Reproducibility of the refractive index data was within 1×10^{-4}.

Preparation of Aqueous Solutions of NFM and Salt Solutions. Binary mixtures of NFM and deionized distilled water were prepared by mass. The weight percentage error is estimated to be less than 0.1%. Salt solutions were made by weight with use of a four-place digital balance. Stock solutions of KI in each concentration of NFM–water binary mixtures were prepared by direct weighing, and these were diluted accurately by using previously calibrated glassware to obtain different required concentrations.

Results and Discussion

The obtained densities, viscosities, and refractive indexes of the aqueous solution of NFM and the solutions of KI in NFM–water mixtures at 25, 35, and 45 °C are listed in Tables I and II. The viscosity behavior of aqueous solutions of NFM shows a negative deviation from ideality (Figure 1). The viscosity of the solution of KI in NFM–water shows an ideality for mixtures containing from 0 to 50 wt % NFM, and when the concentration of NFM increases, the viscosity behaves negatively toward ideality (Figure 2).

The Jones–Dole *B* coefficients were calculated from the slope of the linear regression of the following equation (*5*).

$$(\eta/\eta_0 - 1)/C^{1/2} = A + BC^{1/2}$$

where η is the viscosity of the solution of KI in the NMF–water mixture and η_0 is the viscosity of the mixture of NFM–water only. *A* and *B* are the characteristic parameters for the salt and solvent depending on ion–ion and ion–solvent interactions, respectively, and *C* is the molar concentration of KI in NMF–water mixtures. The Jones–Dole *B* coefficients are listed in Table II and plotted versus the weight percent of NFM in Figure

0021-9568/92/1737-0158$03.00/0